

Electroplated Nanocomposites of High Wear Resistance for Advanced Systems Application

Ioury Timoshkov, Victor Kurmashev and Vadim Timoshkov
*Belarus State University of Informatics and Radioelectronics
Belarus*

1. Introduction

Micro and nanosystems have become the integral part of human being. They help people to improve safety, health and quality of life. Such modern complex advanced systems and their production technologies require new types of material to be developed. These materials should be structured by shape and properties in nano and micro scale for fulfilment of requirements and further incorporation into the systems.

One of the approaches to solve the problem of wear and friction of mechanically moving and load carrying elements of micro and nano dimensions is the use of nanocomposite materials; in particular, codeposited metal and alloy with inert hard nanoparticles by electrochemical or electroless processes. Composite coatings have unique properties that not typical for each phase apart. Varying metal matrix and second dispersed phase the following properties of composite coatings can be improved: hardness, wear-resistance, coefficient of friction, and corrosion-resistance and exposure endurance to aggressive environments. Synthesis of composite coatings by electrolytic codeposition is promising in terms of its low cost, simplicity, and adaptability for different industrial processes. The most exciting applications of plated nanostructured materials are microelectromechanical systems (MEMS), roll-to-roll polymer and nanoimprint technologies. Friction, wear and failure resistance of functional layers are fundamental problems and determine their lifetime.

2. Nanocomposite plating process

Nanocomposite coatings containing ultra-fine particles were plated from sulphate, glycine, acetic, and Watts bathes. Soft magnetic (NiFe, CoFeP, CoP) and hard magnetic (CoNiP, CoW, CoP) alloys as well as conductive matrix of Cu and Ni were investigated. The thickness of the investigated deposits was up to 200 μm . Concentration of ultra-fine particles was varied from 0 to 10 $\text{g}\cdot\text{dm}^{-3}$ (dry substance). Diamond, alumina and aluminium monohydrate ultra-fine particles and BN microparticles were used (Fig. 1).

Average size of nanodiamond particles was 7 nm, alumina - 47 nm, aluminium monohydrate - 20 nm and boron nitride - 1 μm . Codeposition process was carried out in the electrolytic cell of flow type (Fig.2).

Nickel coatings are deposited from the bath: nickel sulfamic-acid water - 400-420 g/l, boric acid - 35-40 g/l, saccharin sodium salt - 0,5-1 g/l, surfactant - 0,2-2 g/l, ultra-dispersed particles - 2-10 g/l, temperature - 38-42 $^{\circ}\text{C}$, current density - 2,2-2,5 A/dm^2 , pH - 4,0-4,2.

Deposition rate is 30 $\mu\text{m}/\text{h}$. Optimal concentration of ultra-dispersed particles is defined experimentally: Al_2O_3 - 4,0 g/l; UDD - 2,0 g/l, AlOOH - 5,0 g/l

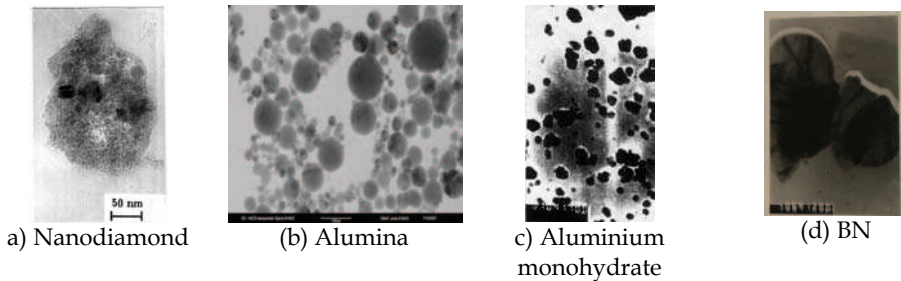


Fig. 1. Inert particles used for codeposition.

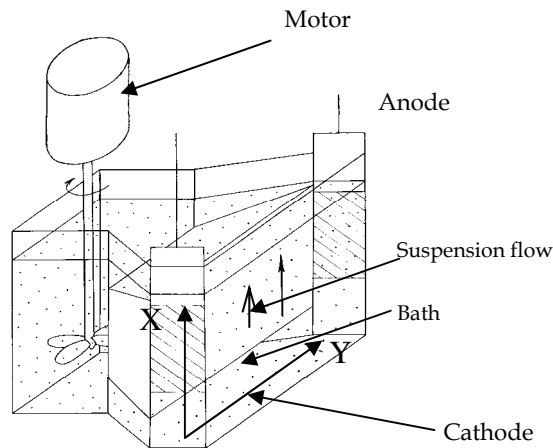


Fig. 2. Electrolytic cell for codeposition process.

The amount of codeposited particles was determined both by integral Coulometric analysis on express analyser AH-7529 (USSR) and by local Auger spectroscopy (PHI-660 Perkin Elmer Corp., USA). The Vickers microhardness of coatings was measured at a load of 0.5 N with MICROMET-II (Buehler-Met, CH). The structure of the deposits was explored by TEM (EM-125, USSR). The coefficient of friction and the wear were evaluated by a FRETTING II test machine (KU Leuven, BE). Wear volumes were estimated by RM600 laser profilometry (Rodenstok, D) after 100,000 fretting cycles.

3. Codeposition model of nanocomposite plating

In general, during the electrolytic codeposition, the suspended inert particles interact with the surface of the growing film due to hydrodynamic, molecular and electrostatic forces (Fransær et al. 1992). This complex process results in the formation of composite coatings.

Auger profiles (Fig.3) and local X-ray analysis (Fig.4) demonstrate that ultra-fine particles are effectively incorporated into the meal matrix.

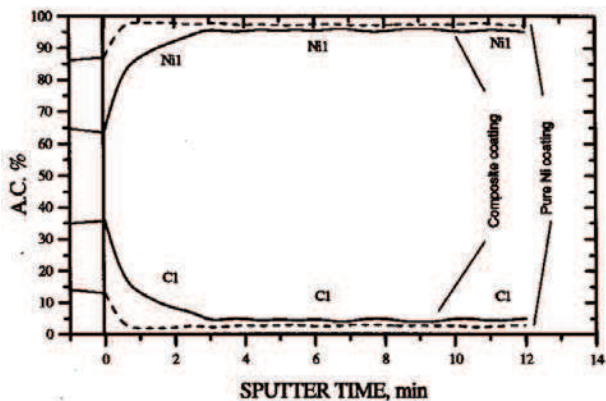


Fig. 3. AES sputter-etch elemental profiles of pure and composite with nanodiamond Ni coatings.

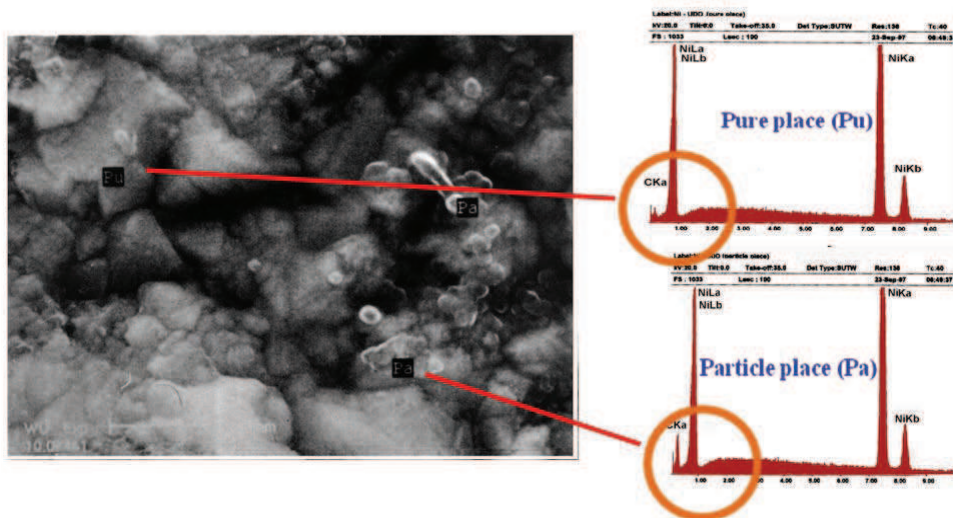


Fig. 4. SEM image and local X-ray analysis of composite Ni-nanodiamond coating.

Based on the experimental data (Timoshkov et al. 1999), the qualitative codeposition model of the composite coatings with the ultra-fine particles was suggested. The peculiarities of the ultra-fine particles behaviour are considered in the model. The model worked out is based on the assumption the codeposition of ultra-fine particles proceeds through the following stages (Fig.5):

- coagulation of ultra-fine particles in plating solution,

- formation of quasi-stable aggregates and therefore change of system dispersion constitution,
- transport of the aggregates to the cathode surface by convection, migration and diffusion,
- disintegration of the aggregates in the near-cathode surface,
- weak adsorption of ultra-fine particles and aggregate fragments onto the cathode surface,
- strong adsorption of dispersion fraction (embedding).

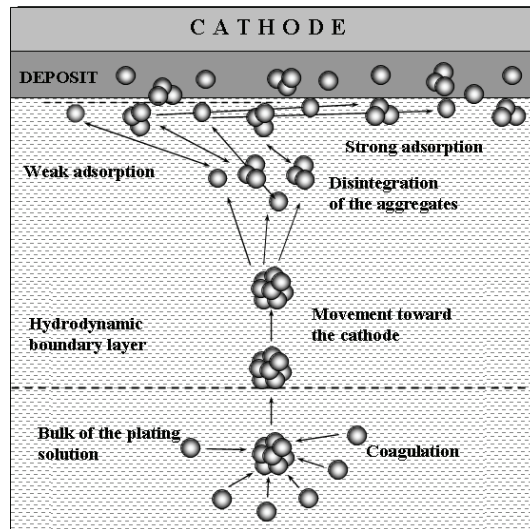


Fig. 5. Model of nanoparticles codeposition process.

Hydrophobic colloidal systems are thermodynamically unstable due to the surplus of the surface energy. They exist owing to stabilization by protective ionic and molecular layers. In general, in the bulk of suspension the particles encounter one another because the Brownian movement, gravity and convection. The forces between them determine whether the encounters result in sticking the particles or the particles remain free.

Behaviour of dispersed systems is described by DLVO theory. Stability or coagulation rate of suspensions depends on sign and magnitude of overall potential energy of interaction between the particles. Positive electrostatic repulsion energy $U_r(h)$ decreases by exponential law, whereas negative molecular attraction energy $U_a(h)$ is inversely proportional to squared distance. As a result, at small distances ($h \rightarrow 0$, $U_r(h) \rightarrow \text{const}$, $U_a(h) \rightarrow -\infty$) and large distances (exponent diminishes much rapidly than power function), the attraction energy between the particles prevails. The electrostatic repulsion energy prevails at intermediate distances. The primary minimum 1 corresponds to direct sticking of particle. In this case, the particles are irreversibly stuck (coalescence). The secondary minimum 2 corresponds to attraction through interlayer of environment. In this case, the aggregates may be counteracted relatively easily. The maximum corresponding to intermediate distances characterizes the potential barrier, which prevents sticking the particles. Forces of interaction are extended for hundreds of nanometers.

In the consideration of interaction between the particles, the following conclusions from DLVO theory should be mentioned as well. The height of the energy maximum and the depth of the primary and secondary maximum depend on the parameters of the systems, namely the zeta potential, particle size, electrolyte concentration (and valence) and the Hamaker constant. At low electrolyte concentration, the energy maximum may reach high values and this prevents particle aggregation. At increase of the electrolyte concentration, the height of the energy maximum decreases and disappears at a critical concentration (which depends on valence of electrolyte). The coagulation becomes more rapid. Thus, to enhance the suspension stability, one needs to reduce the electrolyte concentration and increase the zeta potential.

The transport of the particles toward the cathode surface occurs by convection, migration, diffusion, and Brownian movement.

Migration is the movement of cations, anions or charged particles through the solution under influence of applied potential between the electrodes in that solution. *Diffusion*. Electrode reaction deplete the concentration of oxidant or reluctant at an electrode surface and produces a concentration gradient there. This gives the rise to the movement species from the higher to the lower concentration. Unlike migration, which only occurs for charged particles, diffusion occurs for both charged and uncharged particles. *Convection* includes thermal and stirring effects, which can arise extraneously through vibration, shock and other types of stirring and temperature gradients. *Brownian movement*. It is known, the Brownian movement is affected strongly by the particle size, and may be neglected in the case of the particles size is above 1 μm .

Stirring mode is required to be the transition mode between the turbulent flow and the laminar flow in the bulk of plating bath. Such a mode is of most practical significance. It is because the laminar flow does not provide the sufficient stirring of the electrolyte-suspension. Alternatively, at the stirring rate corresponding to the turbulent mode, the conditions preventing totally the particles embedment appear.

In the near-cathode region, the aggregate is influenced by the forces of different nature and direction. Motion of the aggregate is determined by resultant force, and integrity of aggregate – by sum of forces values as well. For the investigated system, the following forces are considered:

- mechanical forces, associated with interaction with the fluid flow and other particles, gravity and buoyancy;
- electrical forces, connected with the electric field that presents in the plating solution during electrodeposition process;
- molecular forces acting on the particle in the vicinity of the cathode surface.

Mechanical forces. At the laminar liquid flow in the boundary hydrodynamic layer the law of viscous friction is followed in this region, and the boundary conditions are following: $V=0$ at $y=0$ and $V=V_0$ at $y=\infty$.

If the particle moves in the flow having transverse velocity gradient of liquid movement the rotation motion can be imparted to the particle because the different velocities of flow past a particle from the top and from the bottom. The transverse particle migration appears as the result of the rotational motion. The transverse particle migration results from pressure drop on the side where the sum of the tangential velocity components of flowing past and rotating the particle reaches the maximum. The transverse particle migration is directed always toward this maximum. In the case being considered particle moves away from the

cathode surface. When the particle is trapped by cathode, the longitudinal force by flow of the plating solution affects the particle. If this force exceeds the friction force keeping the particle onto the cathode surface, the particle is detached from the growing deposit.

Besides the forces connected to interaction between the particle and hydrodynamic flow, the gravity and buoyancy contribute to particle motion. The sum of forces by gravity and buoyancy results in the sedimentation force.

Collisions between the particles in the near-cathode region may change the particle trajectory promoting or preventing the particle movement to the cathode. Moreover, the particle in the electrolyte may collide with the particle trapped by the cathode and prevent embedment.

Electric forces. The ions in the double layer around the particle interact with the electric field in the plating solution. This results in the particle motion along the lines of electric field. The motion is affected by the fluid permittivity, particle size, intensity of electric field in the particle place, and zeta potential. Sign and value of zeta potential is determined by both the particle nature and the electrolyte constitution and can be changed by addition of surfactants into the plating solution. In the near-cathode region, the cathode itself affects ambiguously the electrophoretic particle motion. On the one hand, modification of the electric field lines in the near-cathode region slows down the particle movement, and on the other hand, the cathode surface itself increases the intensity of the electrophoretic movement. It should be emphasized that it is not possible measurement of zeta potential in the near-cathode region because it depends on many factors and can change not only its value but the sign as well. Therefore, it is difficult task to evaluate the contribution of electrophoretic particle motion into the codeposition process.

In the near-cathode region, the osmotic pressure of the electrolyte affects the particle motion. The electroosmotic motion is the phenomenon of liquid movement through porous body under application of electric field. Assuming the particles in the near-cathode region as a porous bodies, the ionic species move through this "body" due to electric field in the plating solution. In its turn, the ion flow exerts the pressure upon the particles and assists the particle movement toward the cathode surface. It should be mentioned that the electroosmotic motion of particle is influenced by those parameters as for electrophoretic motion (see above).

Molecular forces. At the immediate vicinity of a cathode surface the van der Waals attraction force appears. It occurs with all types atoms or molecules. It arises from the charge fluctuations within an atom or molecule that is associated with the motion of its electrons. A strong repulsive force appears at short distances, when the electrolyte concentration exceeds a certain value. This force is called the structural or hydration force. It originates from the fact that the thin solvent layer presents near the interfaces. This solvent layer is ordered by hydration of cations adsorbed onto surfaces as the interfaces approaches each other. The hydration force results from change in the structure of solvent between the interfaces and prevents the interfaces from close approach.

As particles aggregate approaches the near-cathode region, the force field increases. If these forces exceed a certain critical value, which keeps the particles in the aggregated state, the aggregates are disintegrated. Further, the solitary particles and the aggregate chips interact with the cathode and can be adsorbed weakly onto the cathode. The weak adsorption step assumes the interaction between the particle and cathode surface through adsorbed layers of ions and solvent molecules. Further, the electric field helps to uncover the particle. The thin

interlayer between the cathode surface and particle disappears. It leads to strong field-assisted adsorption and the particle is overgrown with deposit.

A structural investigations confirm proposed model of heterogeneous nanocomposite coating formation. Fig.6 shows that pure Ni coatings contain twins, dislocation aggregates inside the grains, and a concentration of solitary dislocations and dislocation walls of 20 nm thick along the grain boundaries. The average grain size is about 500 nm. As for nanocomposite coatings the grain size reduces up to 30-100 nm. An accumulation of ball-type dislocations along the grain boundaries takes place. Thus, for the first time it was determined that during codeposition of matrix and nanodiamond particles, nanocrystalline Ni electrodeposits were formed.

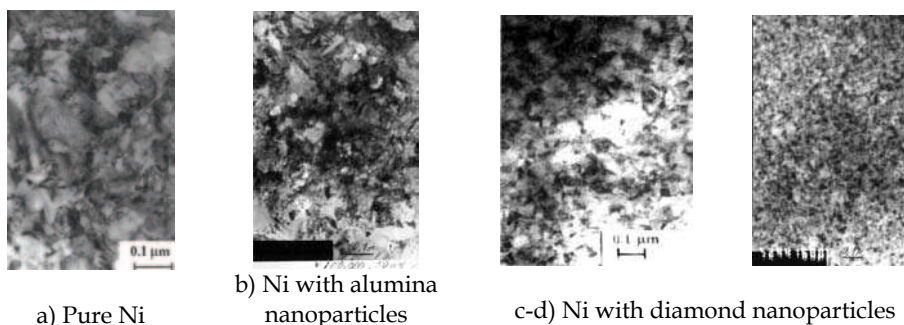


Fig. 6. TEM micrographs of pure Ni and nanocomposite coatings

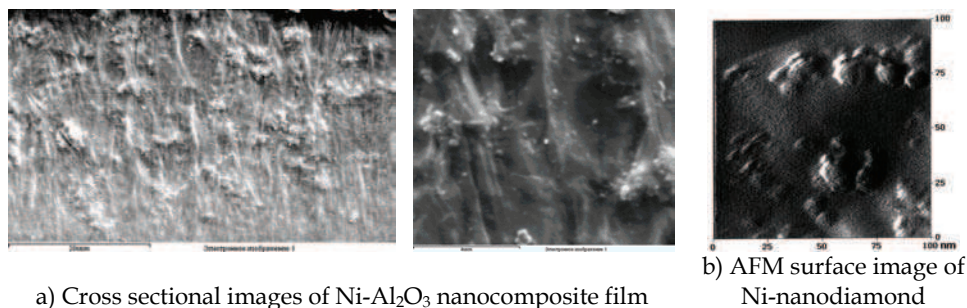


Fig. 7. SEM and AFM images of nanocomposite materials

Cross-sections show that ultra-fine particles are effectively incorporated into the metal matrix (Fig.7). These nanoparticles are distributed in the matrix volume uniformly. Small fragments of aggregates and separate nanoparticles form heterogeneous structure of nanocomposite.

4. MEMS based nanocomposite elements

Micro and nanosystems are the completed devices that combine into one sensor, electronic, and mechanical parts. Mechanical interaction between nano-, micro-, and macro world is the limiting factor for such a complex system. Three dimensional moveable structures should be

integrated in micro and nanosystems from design and technology perspective. Moreover, in general reliability of the systems is determined by the reliability of the mechanical part. Fig. 8 shows that as MEMS become more complicated and for the implemented tasks of higher level, increasing the capability to data processing, improving the sensitivity and possibility to generate mechanical response to some action, the number of the elements should be increased and reaches 10^9 for both electronic and mechanical elements.

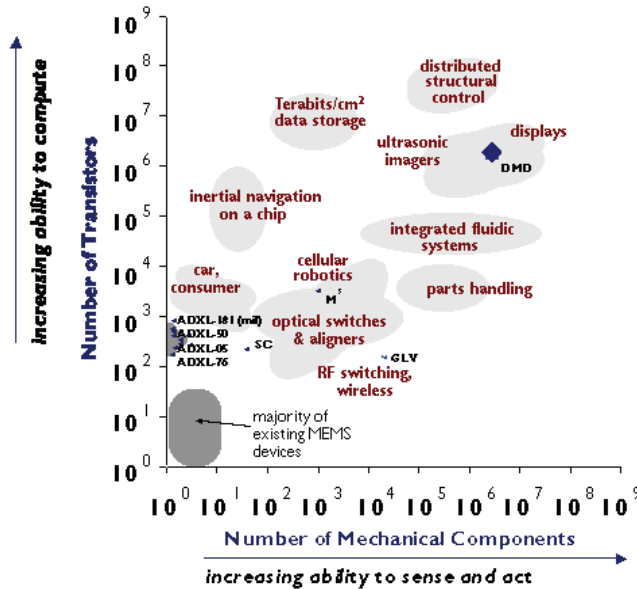


Fig. 8. Progress trend and interdependence of electronic and mechanical parts of MEMS (Pan, 1999).

Technologies of microelectronics have developed and improved for ten years, and at present they achieve perfection. On the other hand, mechanical elements of MEMS require the special design and technology methods to be developed. It is necessary to point out, that upon the movement from pure scientific investigation to practical use of the systems, the reliability are of the great importance. For present stage of MEMS/NEMS development mechanical elements possess significantly lower reliability in comparison with electronic ones and, consequently, reliability of the systems is determined by the reliability of the mechanical part namely.

LIGA (Lithografie, Galvanoformung, and Abforming) technology is the well-known classical process to produce mechanical microelements for MEMS (Fig.9). The main stages of the LIGA process are: obtaining 3D mould of the element with high aspect ratio; metal (alloy) deposition into the form by plating methods; removing the mould to release the elements.

In terms of functionality, the most important properties of the micromechanical elements are friction and wear resistance. Codeposition process instead pure metal (alloy) plating allows increasing reliability of the elements and MEMS in general significantly. For nanocomposite systems, the mechanical properties are determined by the phase composition of the

materials, i.e. by the matrix-to-particle content ratio. Increase of particles concentration in electrolyte influences on increase of foil microhardness slightly. Fragility increases significantly. It deteriorates reliability during exploitation.

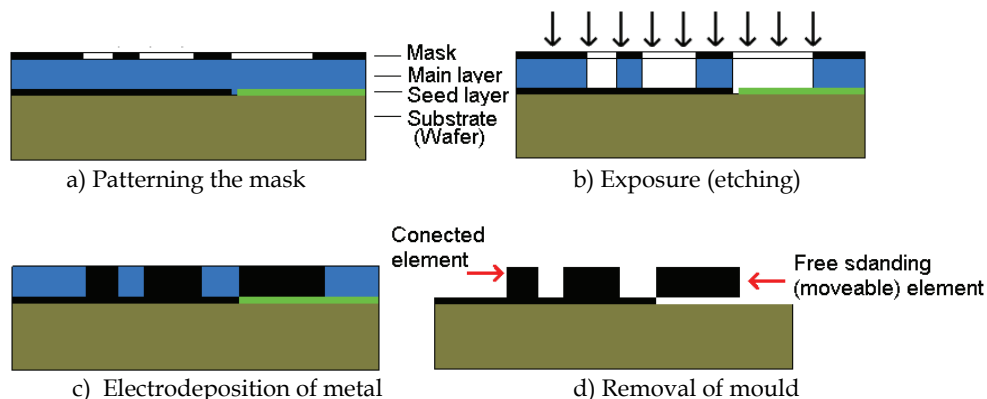


Fig. 9. Process flow of LIGA technology.

One of the main characteristics of nickel deposits is internal stress. Big stress can be reason of crack formation at deposition process or operation. Strain and compressing stress is typical for nickel deposits. Sign of stress to a great extent depends on dopes in electrolyte. Its value is up to nature of electrolyte. Deposits from sulphate electrolyte has high internal stress, while from sulphamate electrolyte - small stress [9]. Internal stress in nickel deposits depends on concentration of basic components in electrolyte. It's determined that tendency to decrease internal stress to zero with following transfer to compressing tensions is observed in sulphamate electrolyte with concentration change of nickel salt from 100 till 800 g/l. Significant change was in concentration range 350-650 g/l. Boric acid don't influence almost on properties of nickel deposits. Variation of pH in solution has big influence on value of internal stress. Minimum of stress displaces to range of higher pH with lowering of nickel amidosulfate concentration. Internal stress of deposits decreases with increase of electrolyte temperature. There is small stress at deposition temperature 60°C. It can be explained by crystal enlargement at high temperature.

Hardness of nickel deposit depends on nickel amidosulfate concentration slightly. But it changes noticeably with increase current density and pH of electrolyte. It can be explained by structural changes of deposit. Structure refinement is observed at increase of pH. It goes with increase of hardness. Hardness decreases sharply at high current density. It increases insignificantly at current density 1-5 A/dm². Hardness of nickel deposits reduces on 15-20 per cent with increase of electrolyte temperature from 20 till 60 °C as a result of enlargement of its structure. Hardness increases at addition in electrolyte organic additives, which promote to refinement of structure. These additives are saccharin, benzenesulphide, propargyl alcohol. Hardness can be increased till 600-700 kg/mm² by codeposition nickel with ultradispersed particles..

Among the coatings tested, composite nickel coatings containing ultra fine diamond particles show a lower coefficient of friction. The amount of particles in the coatings affects the wear rate (Fig.10). The wear volume for pure Ni and composite coatings is shown for fretting tests performed with 100,000 cycles (Fig. 11).

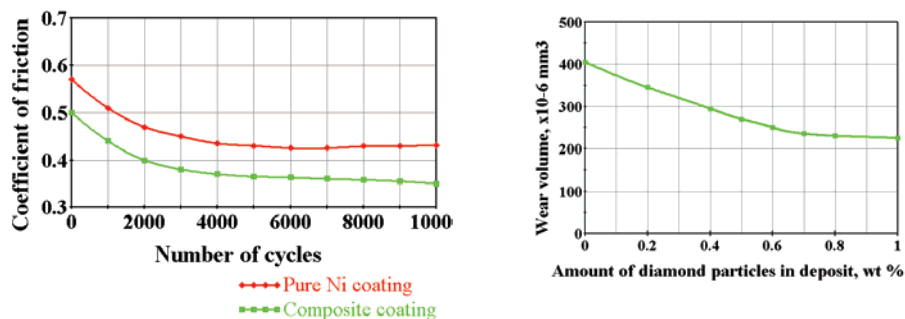


Fig. 10. Coefficient of friction and wear volume for pure and nanocomposite Ni.

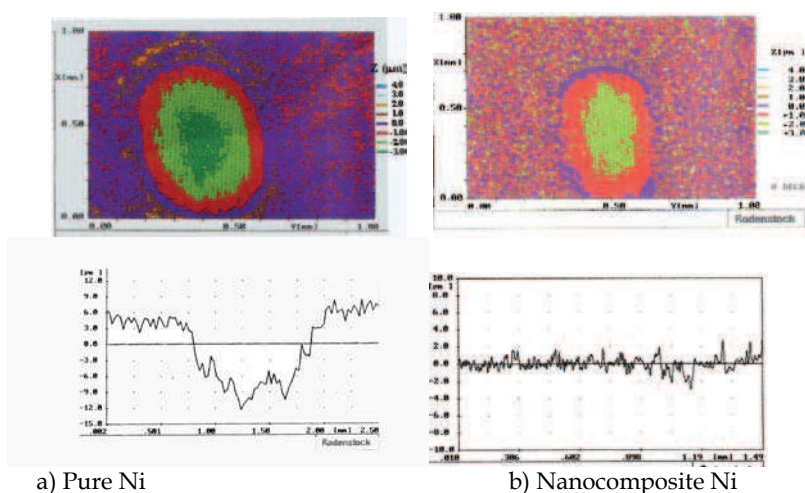


Fig. 11. Light profilometry and position-depth profiles of fretting scars after 100,000 cycles.

The amount of particles in the coatings affects the wear rate. The friction behaviour of multiphase materials has been described in the literature (Mezlini and et al., 2009). The main problem with these approaches is that they are static ones and applied to ideal surfaces because during wear of a multiphase material the topography changes in practice continuously. Localised wear of the matrix takes place in the first phase. After that, the particles become more loaded. This dynamic process may lead to an increased wear resistance of composite materials. Of course, the fretting wear properties of composite coatings are also influenced by the size, shape and distribution of the reinforcing phase. Some MEMS nanocomposite LIGA elements for different types of micromotors were produced and tested (Fig.12).

Friction, wear and corrosion are the key problems for MEMS with real mechanically moveable elements. Codeposition processes allow getting nanocomposite elements with high operate reliability: wear resistance increased in 2-2.5 times, microhardness increased in 2 times, coefficient of friction and corrosion current were reduced factor 1.5 and 1.6 respectively. Developed technologies were tested on prototypes of the electromagnetic and pneumatic micromotors.

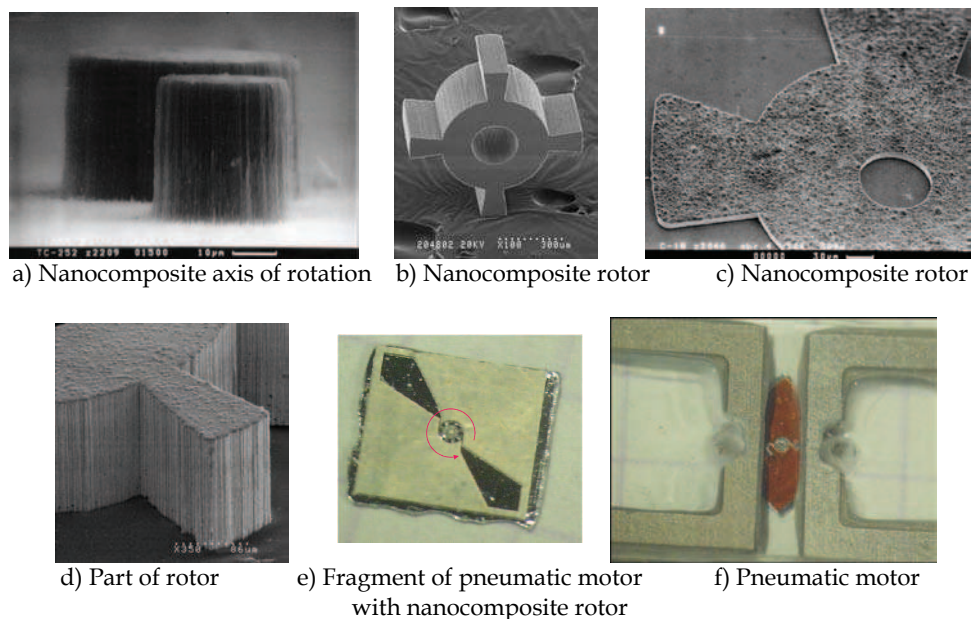


Fig. 12. Nanocomposite MEMS elements.

5. Nanocomposite materials for roll-to-roll and nanoimprint technologies

Gordon Moore projected that the number of components per chip would reach a doubling every two years (Moore, 1975). And the prediction is not going to stop soon. Modern semiconductor industry is following this trend for more than 45 years. And according to International Technology Roadmap for Semiconductors (ITRS) in 2011 28nm halfpitch node is going to be introduced for high volume manufacturing (HVM) in flash memory as main driver for technology shrinkage (<http://www.itrs.net>).

Modern lithography supports a Moore’s law to enable further shrinkage of feature size. As habitual immersion 193nm lithography is approaching its resolution limit, lithography R&D needs new techniques to step into 1x technology node. Candidates for future nanopatterning technologies are extended Double Patterning (DP) (Noelscher et al., 2009) with ArF immersion lithography, extreme ultraviolet (EUV) lithography, multi electron beam lithography (EBL) and nanoimprint lithography (NIL). Each approach has own advantages and disadvantages. At 1x node DP, EUV and EBL would have low throughput with high cost per layer. NIL in comparison with competitors offers sub-10 nm resolution, high-throughput and low-cost patterning, and has a chance to be next generation lithography in future HVM.

Nanoimprint lithography was invented in 1995 by Prof. Stephen Y. Chou (Chou et al., 1995). Schematic NIL process is presented on Fig.13. In that faraway time he demonstrated a feasibility of printing 25nm contact holes, vertical and smooth sidewalls, and nearly 90° corners. Similar technology requirements are going to be used in production soon.

As it is shown on fig.13 a mould is pressed into a thin thermoplastic polymer film that is heated above its glass transition temperature. At this temperature the polymer behaves as a

viscous liquid. It can flow under a pressure and fully repeat the mould. After cooling down resist is hardened and the mould is removed from the substrate. Pattern could be transferred into underlayer by etching process. Quite simple principle of operation makes NIL tools cheap, fast and reliable.

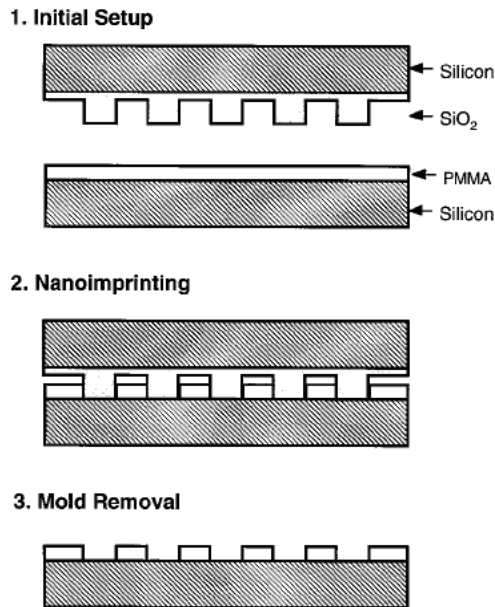


Fig. 13. Schematic of nanoimprint lithography process.

There are many different types of NIL processes, but three schemes are important: soft-lithography, thermoplastic nanoimprint process and resist-dispense photo nanoimprint process (Choi, 2010).

The template for soft lithography is made with a very flexible material (Xia et al., 1998). For example, in micro-contact printing (μCP) 'ink' adhered to features on a template is transferred to a substrate using contact of the inked template and the substrate. This layer acts as an etch mask for subsequent etch processes.

In photo nanoimprint lithography a low-pressure of template and room temperature process is achieved due to the use of a low-viscosity UV-curable resist. The resist is dispensed in picoliter drops over the printing area. With low pressure the template is placed on the substrate, and subsequent UV curing induces cross-linking in the resist material. The transparency to UV light is required from template material, what significantly reduce the list of possible materials.

Thermoplastic nanoimprint lithography possesses sub-10 nm replication resolution and has the most attractive cost per layer. Principle of thermoplastic nanoimprint lithography mentioned above, where the template is in contact with a high viscosity spin-coated resist. There is no material restriction for templates, so wide range of materials can be used: metals, dielectrics or semiconductors. Application of nanocomposite materials could improve reliability of this process.

Also some other types of NIL are in the interest of research groups, such as nanoimprint with incorporation of carbon nanotubes (CNT) (Choi et al., 2008), electrochemical nanoimprint (Hsu et al., 2007) and laser assisted direct imprint (Chou et al., 2002).

Manufacturing requires a high throughput to production equipment. To obtain very high throughput with modest resolution an alternative approach to flat NIL - roller nanoimprint lithography (R-NIL) has been proposed (Tan et al., 1998). Compared with basic flat thermoplastic NIL, R-NIL has the advantage of better uniformity, less force, and the ability to repeat a mask continuously on a large substrate. Two methods of roller nanoimprint were presented: imprint using a cylinder mold by mounting a master mold of cylinder shape around the roller, and imprint using a flat mold by putting the mold directly on the substrate and rotating the roller on top of the mold. Roller nanoimprint tool was developed by Hitachi Ltd. (Fig.14) (<http://www.hitachi.com>).

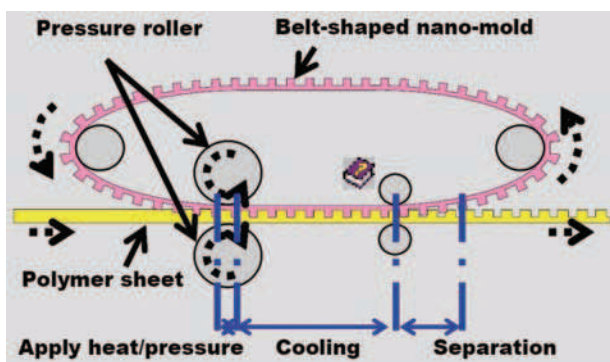


Fig. 14. Schematic diagram of roller nanoimprint tool presented by Hitachi in 2006.

The key concerns for nanoimprint lithography are template patterning, overlay, defects and template wear. Mask patterning requires 1x scale to printed pattern and could be made by means of e-beam and ion-beam lithography. But that's making mask writing at high resolution quite expensive. Due to heat-cool cycles of the template and high pressure compression into resist, it is very difficult using thermoplastic NIL to effect nanoscale alignment and overlay of printed structures as needed in semiconductor device manufacturing.

But the main problem of NIL is low robustness of template due to high pressure of pressing, and it leads to high defectivity level. However, the use of amorphous metals (metallic glasses) (Kumar et al., 2009) and nanocrystalline composite metals and alloys allows to pattern the template on sub-100 nm scale, what can significantly reduce the template cost and improve robustness.

Other issues of NIL, and especially in roller NIL, are resist pattern deformation and fracture during separation process of mask from substrate due to adhesion and friction forces (Wu et al., 2009; Kim et al., 2010).

Usage of bulk nanocomposite templates can improve reliability of NIL processing. Such materials have advantages in comparison with conventional crystalline templates such as good wear resistance, high microhardness, low adhesion, 3D repeatability of mold and low cost of production. The properties of nanocomposite materials are described above in this chapter. Reliability of the conventional templates could be improved by deposition of

antisticking layers, such as diamond-like carbon (DLC) layers, composite chrome coating with nanodiamond particles presented further.

Nanocrystalline structure of composite metal coating allows to resolve sub-100nm features on nanoimprint templates due to its reduced grain size up to 30-100 nm. Test mold structures of 1 μ m wide (Fig.15) are filled with nanocomposite metal material using developed LIGA-like technology. Deposited metal repeats the mold shape.

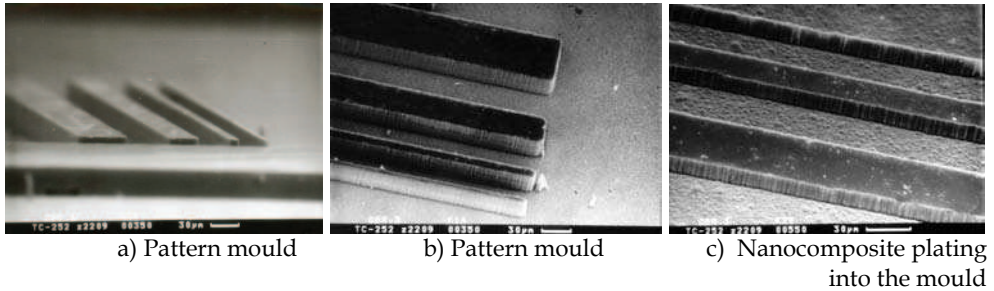


Fig. 15. Test polyimide patterns with minimum feature size of 1 μ m for following plating of nanocomposite metal.

As feasibility of 1 μ m feature transfer from the mold to composite metal template is shown, future activities will be directed to produce sub-100nm metal features. Advantage of the use of nanocomposite materials for roller NIL is proved on example of its application in roll-2-roll technology presented below.

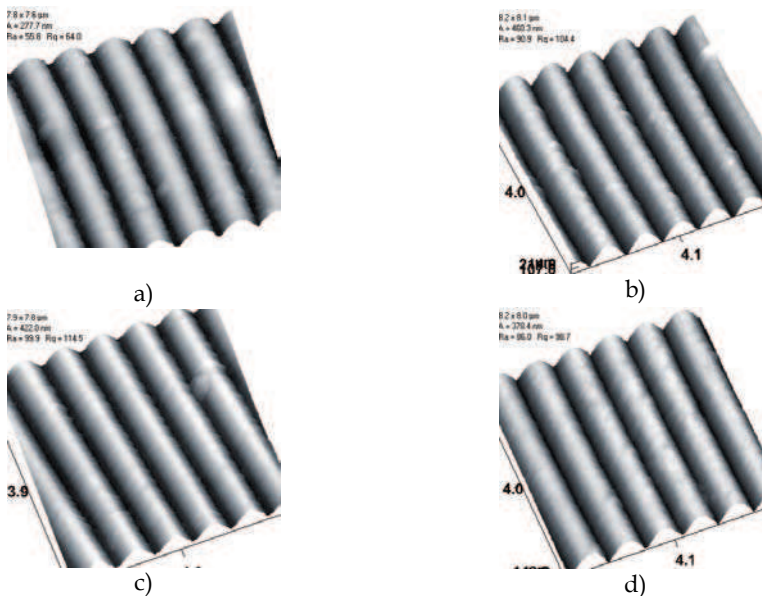


Fig. 16. AFM images of test nanocomposite samples of copies: a – pure Ni, b – Ni with Al_2O_3 , c – Ni with diamond particles, d – Ni with aluminum monohydrate.

Also, high precision galvanoplastic technology is used in holographic industry to produce optical diffraction gratings and images. Roll-to-roll technology is the basis for replication by mechanical pressing of metal matrix into multilayer polymer basis. Working nanocomposite nickel matrix was developed, as well as composite chromium protective coating deposited with nanodiamond particles on top of pure nickel matrix.

Nickel foils are deposited from bath: nickel sulfamic-acid water - 400-420 g/l, boric acid - 35-40 g/l, saccharin sodium salt - 0,5-1 g/l, surfactant - 0,2-2 g/l, ultra-dispersed particles - 2-10 g/l, temperature - 38-42 °C, current density - 2,2-2,5 A/dm², pH - 4,0-4,2. Deposition rate is 30 μm/h. Optimal concentration of ultra-dispersed particles is defined experimentally: Al₂O₃ - 4,0 g/l; UDD - 2,0 g/l, AlOOH - 5,0 g/l. Increase of particles concentration in electrolyte influences on increase of foil microhardness slightly. Fragility increases significantly. It deteriorates reliability during exploitation.

Patterned grating copies and gratings before and after test are shown on Fig. 16 and 17 respectively. They have been tested by stamping method on 2000 m aluminized lamsan tape. Test results show the increase of holographic matrixes runability on 60-400% with improved printed image quality.

Application of composite materials in NIL and roll-2-roll process is the right way to solve issues and improve reliability of templates and whole technology at all. It helps to bring NIL into HVM, and especially for roller NIL to get even higher throughput than step-and-print nanoimprint lithography.

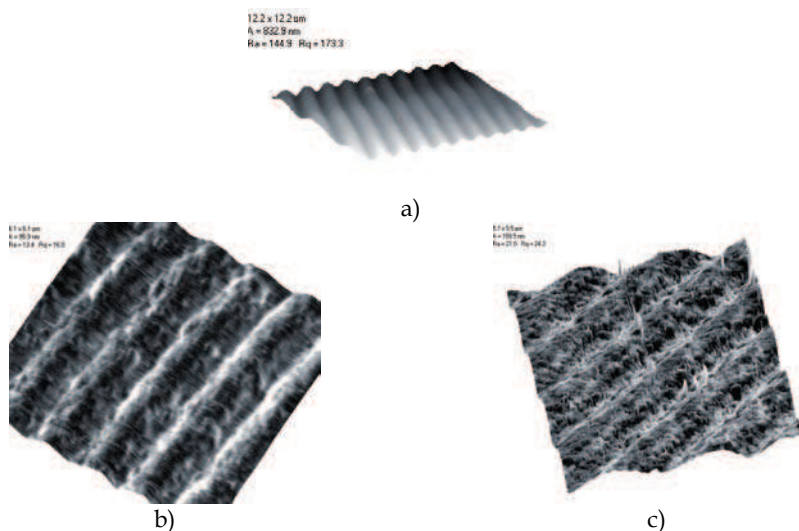


Fig. 17. Reliefs of grating copies before (a) and after test (b,c).

6. Conclusion

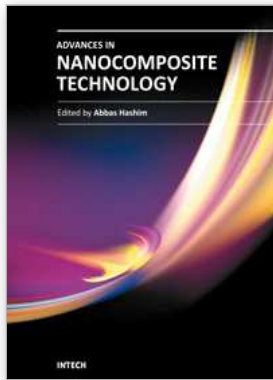
This chapter describes positive consequences of introduction of the nanocomposites in the advanced technologies. Application of nanocomposites in MEMS, NEMS, NIL and roll-2-roll technologies makes it possible to improve quality and reliability of these processes and end products.

Nanocomposite technology may be integrated in the systems technology by replacement of homogeneous pure materials by heterogeneous nanocomposites. This allows to improve set of physical mechanical properties, such as wear resistance, microhardness, corrosion resistance and friction coefficient. Nanocrystalline structure of nanocomposites enables to resolve sub-100nm features in NEMS and NIL applications.

Application of such nanocomposite materials is the only way of industrial development for advanced systems and technologies such as moveable MEMS elements, working matrix in roll-to roll and nanoimprint technologies.

7. References

- Choi, J.; Jung, S.; Choi, D.; Jeong, J. and Lee, E. (2008). *Direct soft UV-NIL with resist incorporating carbon nanotubes*, Microelectronic Engineering, Vol. 85, pp. 195-201
- Choi, J. (2010). *Status of UV Imprint Lithography for Nanoscale Manufacturing*, In G. Wiederrecht, Handbook of Nanofabrication. pp. 149-181. Amsterdam: Elsevier B.V.
- Chou, S.Y.; Krauss, P.R. and Renstrom, P.J. (1995). *Imprint of Sub-25 Nm Vias and Trenches in Polymers*. Applied Physics Letters, №67(21), pp. 3114-3116
- Chou, S.Y.; Keimel, C.; Gu, J. (2002). *Ultrafast and Direct Imprint of Nanostructures in Silicon*, Nature № 417 (6891): pp.835-837.
- Fransaer, J.; Celis, J-P. and Roos, J.R. (1992). *Analysis of the electrolytic codeposition of non-Brownian particles with metals*, Journal of The Electrochemical Society, 139 (2) (1992), pp. 413 -425.
- Hsu, Keng H.; Schultz, Peter L.; Ferreira, Placid M. and Fang, Nicholas X. (2007). *Electrochemical Nanoimprinting with Solid-State Superionic Stamps*, Nanoletters Vol. 7, No. 2 pp. 446-451
- Kim, Kwang-Seop; Kim, Jae-Hyun; Lee, Hak-Joo and Lee, Sang-Rok (2010). *Tribology issues in nanoimprint lithography*, Journal of Mechanical Science and Technology № 24 pp. 5-12
- Kumar; Tang, Hong X. and Schroers, Jan (2009). *Nanomoulding with amorphous metals*, Golden, Nature №457, pp. 868-872
- S. Mezlini, S; and others (2009). *Correlation Between Tribological Parameters and Wear Mechanisms of Homogeneous and Heterogeneous Material*. Tribology Letters Volume 33, Number 2, pp.153-159.
- Moore, G. (1975). *Progress in Digital Integrated Electronics*, IEEE, IEDM Tech Digest pp.11-13
- Noelscher, C.; Timoshkov, V. and others (2009). *Double patterning down to $k_1=0.15$ with litho trim*. J. Micro/Nanolith. MEMS MOEMS 8(1), 011005(Jan-Mar 2009)
- Pan, J. (1999). *MEMS and Reliability*. Dependable Embedded Systems, Carnegie Mellon University
- Tan H, et al. (1998). *Roller nanoimprint lithography*. Journal of Vacuum Science and Technology № 16(6), pp. 3926-3928
- Timoshkov, Yu.; Gubarevich, T.; Orekhovskaya, T.; Molchan, I. and Kurmashev V. (1999). *Properties of Ni-composite coating with different type of ultra-dispersed diamond particles*, Galvanotechnology and surface technologies, v.7, 2, pp.20-26, Russia
- Wu, Cheng-Da; Lin, Jen-Fin and Fang, Te-Hua (2009). *Molecular Dynamics Simulations of the Roller Nanoimprint Process: Adhesion and Other Mechanical Characteristics*, Nanoscale Res Lett № 4, pp. 913-920
- Xia, Y. and Whitesides, G. M. (1998). *Soft Lithography*, Angewandte Chemie - International Edition in English № 27, pp. 550-575



Advances in Nanocomposite Technology

Edited by Dr. Abbass Hashim

ISBN 978-953-307-347-7

Hard cover, 374 pages

Publisher InTech

Published online 27, July, 2011

Published in print edition July, 2011

The book "Advances in Nanocomposite Technology" contains 16 chapters divided in three sections. Section one, "Electronic Applications", deals with the preparation and characterization of nanocomposite materials for electronic applications and studies. In section two, "Material Nanocomposites", the advanced research of polymer nanocomposite material and polymer-clay, ceramic, silicate glass-based nanocomposite and the functionality of graphene nanocomposites is presented. The "Human and Bioapplications" section is describing how nanostructures are synthesized and draw attention on wide variety of nanostructures available for biological research and treatment applications. We believe that this book offers broad examples of existing developments in nanocomposite technology research and an excellent introduction to nanoelectronics, nanomaterial applications and bionanocomposites.

How to reference

In order to correctly reference this scholarly work, feel free to copy and paste the following:

loury Timoshkov, Victor Kurmashev and Vadim Timoshkov (2011). Electroplated Nanocomposites of High Wear Resistance for Advanced Systems Application, Advances in Nanocomposite Technology, Dr. Abbass Hashim (Ed.), ISBN: 978-953-307-347-7, InTech, Available from: <http://www.intechopen.com/books/advances-in-nanocomposite-technology/electroplated-nanocomposites-of-high-wear-resistance-for-advanced-systems-application>

INTECH
open science | open minds

InTech Europe

University Campus STeP Ri
Slavka Krautzeka 83/A
51000 Rijeka, Croatia
Phone: +385 (51) 770 447
Fax: +385 (51) 686 166
www.intechopen.com

InTech China

Unit 405, Office Block, Hotel Equatorial Shanghai
No.65, Yan An Road (West), Shanghai, 200040, China
中国上海市延安西路65号上海国际贵都大饭店办公楼405单元
Phone: +86-21-62489820
Fax: +86-21-62489821

© 2011 The Author(s). Licensee IntechOpen. This chapter is distributed under the terms of the [Creative Commons Attribution-NonCommercial-ShareAlike-3.0 License](#), which permits use, distribution and reproduction for non-commercial purposes, provided the original is properly cited and derivative works building on this content are distributed under the same license.